



ISME

M. Bateni *
M.Sc. Student

M.R. Eslami †
Professor

Optimization of Thermal Instability Resistance of FG Flat Structures using an Improved Multi-objective Harmony Search Algorithm

This paper presents a clear monograph on the optimization of thermal instability resistance of the FG (functionally graded) flat structures. For this aim, two FG flat structures, namely an FG beam and an FG circular plate, are considered. These structures are assumed to obey the first-order shear deformation theory, three-parameters power-law distribution of the constituents, and clamped boundary conditions. The objectives of the optimization problem are considered to be maximizing the critical buckling temperature and minimizing the structural mass. Also, the problems are confined to the range of elastic stability by considering an appropriate constraint criterion. This paper proposes the IMHSA algorithm (improved multi-objective harmony search algorithm) to deal with the stated problem. The capability of the proposed algorithm is examined by solving a benchmark problem. Results are shown as optimal pareto-points for the problems introduced in the paper and some pareto-points are tabulated in detail. Results reveal that the un-symmetric material distribution is not suitable to postpone the buckling temperature of the flat structures.

Keywords: Functionally graded material, Multi-objective optimization, Improved harmony search algorithm, Critical buckling temperature

1 Introduction

The classical composite structures suffer from discontinuity of material properties at the interface of the layers and constituents of the composite. From this point of view, the stress field in these regions creates an interface problem and thermal stress concentration at high temperature environments. Furthermore, large plastic deformation of the interface may trigger the initiation and propagation of cracks in the material. These shortcomings may be decreased by gradually changing the volume fraction of constituent materials. In fact, the FGMs (functionally graded materials) are advanced materials, which have a smooth spatial variation of volume fraction of constituent materials. Due to this spatial variation, mechanical properties of the FG structures in gradation direction have an interesting change. The mentioned characteristic allows the designer to control the critical design aspects, such as maximum effective stress, natural frequency, and structural instability resistance.

Most of real-world engineering optimization problems are multi-objective in nature. This feature exists since for design purposes several objectives may be optimized (minimized or maximized) simultaneously. Usually, these objectives are in conflict with each other, therefore, improving one of them may worsen others. The structural optimization of components made of

* M.Sc. Student, Mechanical Engineering Department, Amirkabir University of Technology

† Corresponding Author, Professor and Fellow of the Academy of Sciences, Mechanical Engineering Department, Amirkabir University of Technology, eslami@aut.ac.ir

the FGMs is not a distinct matter, but it may be considered as a mono-objective optimization problem based on design considerations.

Design of the FG structures as multi-objective/mono-objective optimization problem has been investigated by many researchers. Using direct sensitivity analysis, Tanaka et al. [1] have proposed a macroscopic material tailoring in order to reduce the thermal stresses induced in the FGMs. In this work, a multi-objective optimization without pareto-optimality concepts in conjunction with the FEM have been used for the volume fraction optimization. Ootao et al. [2] have used a neural network for minimizing the thermal stresses in hollow cylindrical vessel. Functionally graded medium in this work has been considered as a sequence of finite numbers of homogeneous layers, then the optimum sequence for reducing the objective function has been obtained. Turteltaub [3], by the Lagrange Multiplier Method, has obtained the optimum material properties for control and/or optimization of a functionally graded composite under a time-dependent thermo-mechanical loading. Cho and Choi [4] have introduced a yield-criteria optimization of the volume fraction distribution. In this study, the objective function has been defined by linearly combining the total strain energy and the peak effective stress scaled by the spatial-varying yield stress. Goupee and Vel [5, 6, 7] have performed a set of works based on the element-free Galerkin method and mono/multi objective real code genetic algorithm. In these works, optimal volume fractions for nodal points have been obtained based on the Mori-Tanaka and self-consistent homogenization schemes. Similarly, self-consistent homogenization scheme and non-dominated sorting multi-objective genetic algorithm have been used by Vel and Pelletier [8]. This paper addresses the optimal nodal volume fractions for functionally graded cylindrical shells under steady thermo-mechanical processes, where the candidate designs have been evaluated by using an analytical power-series solution. Stump et al. [9] have presented a topology optimization framework for minimizing the volumetric density of a material phase subjected to a global stress constraint at micro-level. This work has presented a continuous distribution of the design variable inside the finite element. Xia and Wang [10] have studied the simultaneous optimization of the material properties (via the material volume fractions) and the topology (via the the structural boundaries) of functionally graded structures by using a level-set-based method. Almeida et al. [11], by means of continuous topology optimization and finite element method, have optimized the overall stiffness behavior of functionally graded structures with respect to symmetry and pattern repetition constraints which include material gradation effects at both global and local levels. Vatanabe et al. [13] have proposed a methodology for optimizing energy harvesting applications of functionally graded piezocomposite materials, which is based on topology optimization and homogenization. First natural frequency of three-parameter functionally graded beams have been optimized by Yas et al. [14]. In this work, beam's governing equations have been solved by generalized differential quadrature method, and then nodal volume fractions have been optimized by using an artificial neural network and the imperialist competitive algorithm. Taheri et al. [15] have presented an isogeometrical procedure for optimization of material composition of functionally graded structures in thermo-mechanical processes. In this paper, employing the standard isogeometric analysis method together with the sequential quadratic programming, optimum surfaces of volume fractions as design variables are obtained. Finally, Birman and Byrd [16] presented an interesting literature review about the modeling and optimizing the FGMs.

In literature, the optimization of structures made of FGMs has been preformed in different methodologies and by different solution procedures. One of the main discrepancies between preformed works is modeling of the material distribution thorough the FGM medium and its associated decision variable.

Most of investigations are preformed based on optimizing the volume fraction. This manner

extensively has been used for problems that have no closed-form objective functions. In this manner, point-wise volume fractions, in finite numbers, are decision variables. A wide range of optimization methods are utilized to volume fraction optimization. These optimization methods are powerful to achieve optimal material distributions in the FG structures. However, because of weaknesses in manufacturing process, the optimal material tailoring has not been achieved in practice. To deal with this uncertainty, Noh et al. [17] have performed a reliable design optimization. In their work, the FGM medium is supposed to consist of a finite number of homogeneous layers which have certain volume fractions, and the material properties of those homogeneous layers are considered as decision variables.

Despite of volume fraction optimization, in cases which the core optimizing problem is soluble in an analytical manner, the parameters of FGM models may be selected as decision variables. There are few investigations in this manner. For instance, Loja [18] has studied the application of particle swarm optimization technique in conjunction with a re-initialization strategy for the maximization of bending stiffness of a functionally graded sandwich beam.

Optimization algorithms are another source of discrepancy between performed works on the optimization of the FG structures. The optimization methods can be divided into two main classes; gradient based optimization algorithms and stochastic optimization algorithms. The gradient based optimization algorithms give a directional search in feasible domain of solution vectors and are appropriate for local searching of optimal pareto-points. On the contrary, stochastic optimization algorithms search the whole solution domain for desirable solution vectors. In other words, these algorithms are suitable for global searching of optimal pareto-points.

Each of these main classes and their combinations have been used for optimization of the FG structures. There are some advantages as well as disadvantages in the usage of every class of optimization algorithms. In this condition, efficiency and accuracy of optimization algorithms highly depend on the type and status of optimization problems.

The HS (Harmony Search) is a relatively new meta-heuristic optimization algorithm and it has been firstly developed by Geem et al. [19]. The HS is a stochastic random search algorithm, and it does not need an accurate initial value for converging into the global optimum. Since introducing, this algorithm has been utilized for various design and decision making problems such as structural engineering. Firstly, Lee and Geem [20] have introduced the HS as an algorithm for structural optimization. In most practical structural applications, decision variables must be selected among a set of discrete data. An application and details of the HS for discrete structural optimization have been presented by Lee et al. [21]. The HS was emerged as a mono-objective optimization algorithm. There are many papers in which the mono-objective HS has been employed in order to deal with engineering applications. Among them, Degertekin [22] has used the discrete HS algorithm for minimizing the weight of steel frames with respect to strength and displacement constraints.

Just like all phenomenon-mimicking algorithms, the HS has a set of tuning parameters which are helpful for well-dealing with various engineering problems. Many studies have debated on the setting those parameters with the aim of decreasing in the parameter-dependency and increasing in the accuracy and convergence of the HS algorithm [23, 24]. Applications of different modified HS algorithms have been investigated by Degertekin [25], Gholizadeh and Barzegar [26], and Maheri [27].

Earliest work on the MHS (Multi-objective Harmony Search) was developed by Geem and Hwangbo [28]. In this work, multi-objective optimization for satellite heat pipe design have been studied based on two main steps; 1- each single objective function is optimized, 2- sum of errors between the current function value and the optimal value in terms of single objectives is defined as multi-objective function, then this function is minimized. In a similar manner, Geem

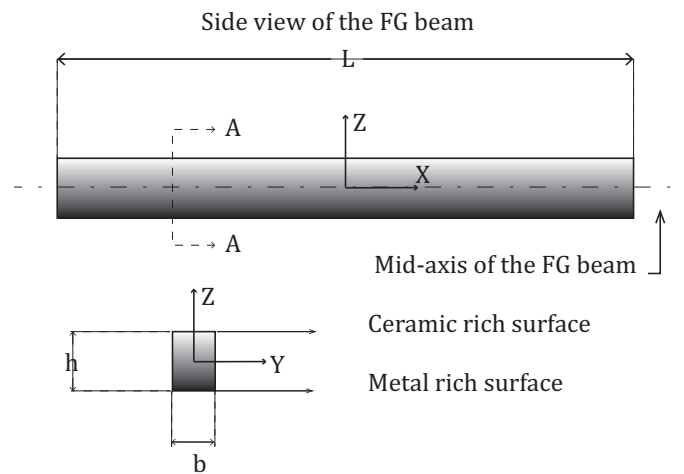


Figure 1 Schematic view of the functionally graded beam and its associated co-ordinate system.

[29] has studied the multi-objective optimization of time-cost trade-off using HS. It should be noted that in the later works, multi-objective optimization have been performed without using *pareto-dominance* concept. For the first time, Ricart et al. [30], by using the pareto-dominance concept, have proposed the MHS algorithm. This paper investigates capabilities of the HS to deal with multi-objective problems in comparison with non-dominated sorting genetic algorithm II. Researches on applications of the MHS based on pareto-optimality concept are not mature and literature on this topic seems to be pure.

The second author has numerous works on the buckling and post-buckling of FG structures under thermal and mechanical loading [31]-[38]. Interesting design facts of the FGMs in conjunction with the capability of the MHS algorithm have motivated the authors to utilize the MHS for optimizing the thermal instability resistance of the FG flat structures. Present study addresses application of the IMHSA to optimize the thermal instability resistance of the FG flat structures. For this purpose, the IMHSA is developed. The accuracy of the IMHSA has been examined by solving the FON test function.

2 Optimizing Structure

Two cases of the FG flat structures are considered in this paper: an FG beam, Fig. (1), and an FG circular plate, Fig. (2). In both model problems, the critical buckling temperature is maximized along with minimizing the structural mass. The solution vectors consist of the power-law index and the thickness of structures. An appropriate constraint function is imposed on the effective stress thorough the structures, so the problems have been confined to the range of elastic stability. The defined optimization problems are solved by the developed IMHSA and illustrative results are presented as the pareto-fronts. Also, some of the pareto-points and their associated solution vectors are tabulated for more details.

3 Core problem

3.1 Modeling of material distribution

The FGMs used herein are assumed to obey the power-law distribution of material properties in one direction. Furthermore, the FGMs are assumed to be composed of two phases, namely;

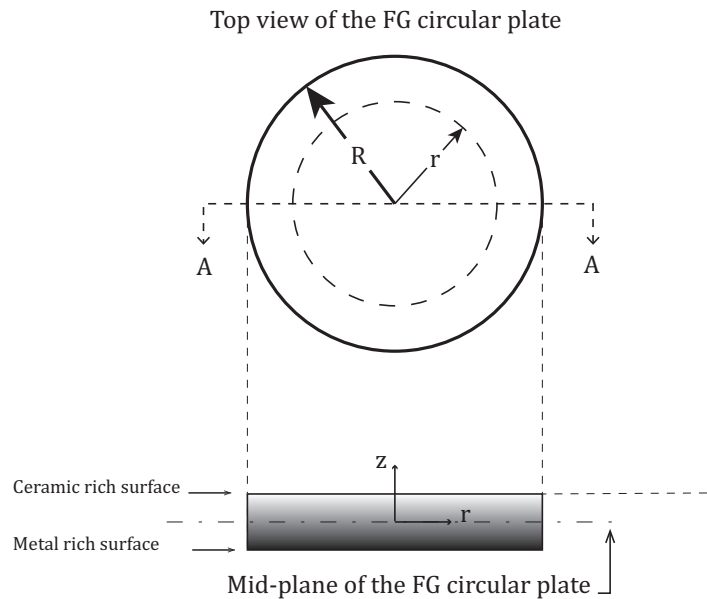


Figure 2 Schematic view of the functionally circular plate and its associated co-ordinate system.

metal phase (subscribe m) and ceramic phase (subscribe c). Now, the volume fraction of constituents may be expressed as Eq. (1).

$$V_c = \left(\frac{1}{2} + \frac{z}{h} \right)^k$$

$$V_m = 1 - V_c \quad (1)$$

where k is the power-law index, z is the coordinate in the gradation direction, and h denotes the thickness in the gradation direction. The material properties of the FGM medium may be defined based on the Voigt rule of mixture and thus the typical material property is

$$P(z) = V_m P_m + V_c P_c \quad (2)$$

Substituting Eq. (1) into Eq. (2) results in Eq. (3) as the distribution of material properties thorough the FGMs.

$$P(z) = P_m + (P_c - P_m) \left(\frac{1}{2} + \frac{z}{h} \right)^k \quad (3)$$

It is known that the precise modeling of FGMs require a deep knowledge at micro-mechanical level and an advanced rule of mixture. Apparently, the Voigt rule presents a rudimentary approximation of material distribution. In this model, the influence of micro-mechanical constraints such as particles shape, particles orientation, particles volume fraction, and so forth are not taken into account. However, the Voigt rule of mixture is broadly used in obtaining the global response of FG structures.

In this work, the thermal buckling analysis of FG structures is performed according to the Voigt rule of mixture but the constraint function imposing on the effective stress of FGMs is derived by another method. The method could be described as follows. Since ceramics are brittle, they have no yield stress at all. Also, the ultimate strength of ceramics is much higher than the yield stress of metals. Therefore, it is assumed that in the ceramic-metal FG medium,

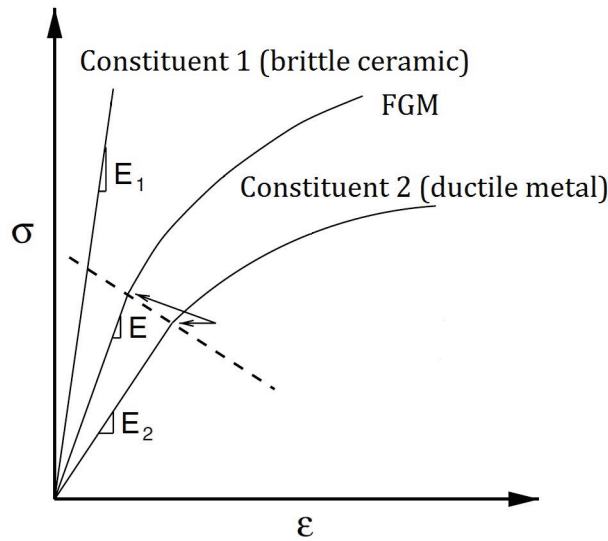


Figure 3 Schematic stress-strain curve for a FGM and its constituents.

the metals reach the yield stress while the ceramics are in the elastic regime. Consequently, for the FGM medium an effective yield strength may be defined. This effective yield strength is a function of the yield stress of the metal phase at each material point, Fig.(3).

Tamura et al. [39] have presented a modified rule of mixture for two-phase alloys. If this rule is adopted for ceramic-metal FG composite [4, 40, 41], the effective yield strength may be obtained as Eq. (4).

$$Y_m < \sigma_y < Y_m \left(\frac{E_c}{E_m} - V_m \left(\frac{E_c - E_m}{E_m} \right) \right) \quad (4)$$

where Y_m is the yield stress of metallic phase and σ_y is the effective yield stress of ceramic-metal FG composite. It must be noted that the lower and upper bounds of the range correspond to the iso-stress and iso-strain conditions, respectively. In other words, the value of effective yield stress could be placed in this range but its exact value is not known. Therefore, in this paper the effective yield stress is assumed to be obtain by Eq. (5).

$$\sigma_y [Mpa] = Y_m \left(\frac{E_c(50000 + E_m)}{E_m(50000 + E_c)} - V_m \left(\frac{E_c(50000 + E_m)}{E_m(50000 + E_c)} - 1 \right) \right) \quad (5)$$

3.2 Objective functions

In this section, the objective functions are derived. The *specific mass* and the *critical buckling temperature* of the FG structures are considered as objective functions.

3.2.1 Specific structural mass

According to the power-law distribution of material properties, density of the FGMs at an arbitrary point can be written in the form

$$\rho(z) = \rho_m + (\rho_c - \rho_m) \left(\frac{1}{2} + \frac{z}{h} \right)^k \quad (6)$$

Integrating Eq. (6) across the thickness direction leads to Eq. (7) as the specific mass of structures per unit area of their mid surface.

$$\rho_{unit} = \int_{-\frac{h}{2}}^{\frac{h}{2}} \left(\rho_m + (\rho_c - \rho_m) \left(\frac{1}{2} + \frac{z}{h} \right)^k \right) dz = h \left(\rho_m + \frac{\rho_{cm}}{k+1} \right) \quad (7)$$

Consequently, for the FG beams the specific mass is

$$m_{bL} = h \left(\rho_m + \frac{\rho_{cm}}{k+1} \right) \quad (8)$$

It is obvious that the total mass of the FG beams may be written as

$$m_{tot}^B = b L m_{bL} \quad (9)$$

where b is the width and L is the length of the beam. Also, for the FG circular plates the specific mass is

$$m_R = h \left(\rho_m + \frac{\rho_{cm}}{k+1} \right) \quad (10)$$

The total mass of the FG circular plates can be defined as Eq. (11).

$$m_{tot}^P = \pi R^2 m_r \quad (11)$$

where R is the radius of FG circular plates.

3.2.2 Critical buckling temperature

Some basic assumptions have been considered in deriving the governing equations of the structures at the buckling configuration. These assumptions are:

- The displacement field of the structures has been assumed according to the first-order shear deformation hypotheses.
- The three-parameters power-law is employed for modeling the distribution of material properties.
- The boundary conditions of the structures are assumed to be clamped.

Based on these assumptions, closed form expressions for the critical buckling temperatures of the considered structures are obtained in previous works [42, 43]. The expressions for the critical buckling temperature of structures are given subsequently.

Model problem 1: FG beams

Consider an FG beam with thickness h , width b , and length L . The critical buckling temperature of the beam subjected to a uniform temperature rise is obtained [42] as

$$\Delta T_{crit} = \frac{r(E_1 E_3 - (E_2)^2)}{L^2 E_\alpha \left(E_1 - \frac{s(E_1 E_3 - (E_2)^2)(1 + \nu)}{K_s L^2 E_1} \right)} \quad (12)$$

where

$$\begin{aligned}
 E_\alpha &= \int_{-\frac{h}{2}}^{\frac{h}{2}} E(z)\alpha(z)dz = h \left(E_m\alpha_m + \frac{E_m\alpha_{cm} + \alpha_mE_{cm}}{k+1} + \frac{E_{cm}\alpha_{cm}}{2k+1} \right) \\
 E_1 &= \int_{-\frac{h}{2}}^{\frac{h}{2}} E(z)dz = h \left(E_m + \frac{E_{cm}}{k+1} \right) \\
 E_2 &= \int_{-\frac{h}{2}}^{\frac{h}{2}} E(z)z dz = h^2 E_{cm} \left(\frac{1}{k+2} - \frac{1}{2k+2} \right) \\
 E_3 &= \int_{-\frac{h}{2}}^{\frac{h}{2}} E(z)z^2 dz = h^3 \left(\frac{E_m}{12} + E_{cm} \left(\frac{1}{k+3} - \frac{1}{k+2} + \frac{1}{4k+4} \right) \right) \quad (13)
 \end{aligned}$$

where $E(z)$ and $\alpha(z)$ are the modulus of elasticity and the coefficient of thermal expansion, respectively. In Eq. (12), parameters r and s specify the boundary conditions of FG beams. For the clamped-clamped boundary conditions these constants are $r = 39.47842$ and $s = 78.95684$. Also, K_s indicates the shear-correction factor associated with the first-order shear deformation assumptions. At the pre-buckling stage, the effective stress at each material point of FG beams can be defined as Eq. (14).

$$\sigma_{eff} = -E(z)\alpha(z)(T(z) - T_0) \quad (14)$$

Model problem 2: FG circular plates

In the second case, consider an FG circular plate of thickness h and radius R . For uniform temperature distribution, the critical buckling temperature of the fully clamped FG circular plate is reported in [43] as

$$\Delta T_{crit} = \frac{14.68(E_1E_3 - (E_2)^2)}{E_\alpha(1 + \nu)E_1R^2} \quad (15)$$

where E_1, E_2, E_3 , and E, α are previously introduced. For the pre-buckling configuration, the effective stress through an FG circular plate may be written as Eq. (16). It should be noted that the plate is under a symmetric thermal loading.

$$\sigma_{eff} = -\sqrt{2} \frac{1}{1 - \nu} E(z)\alpha(z)(T(z) - T_0) \quad (16)$$

4 Optimization problem

The general form of a multi-objective optimization problem is specified as follows

$$\begin{aligned}
 F(X) &= (f_1(X), f_2(X), f_3(X), \dots, f_I(X)) \\
 G_j(X) &= 0 \quad j = 1, 2, 3, \dots, J \\
 H_m(X) &\leq 0 \quad m = 1, 2, 3, \dots, M \\
 L_n &\leq x_n \leq U_n \quad n = 1, 2, 3, \dots, N
 \end{aligned} \quad (17)$$

where I is the number of objective functions, J is the number of equality constraints, and M is the number of inequality constraints. Here, X is the solution vector that is composed of decision variables x_n and N is the number of decision variables. The lower- and upper-bounds of each decision variables are L_n and U_n , respectively. The optimization problems in this article could be defined as

Model problem 1

$$\begin{aligned}
f_1(X) &= m_b L \\
f_2(X) &= \frac{1}{\Delta T_{crit}} \\
\frac{\sigma_{eff}(z)}{\sigma_Y} - 1 &\leq 0 \\
0 &\leq k \leq 20 \\
8 &\leq \frac{L}{h} \leq 80
\end{aligned} \tag{18}$$

Model problem 2

$$\begin{aligned}
f_1(X) &= m_r \\
f_2(X) &= \frac{1}{\Delta T_{crit}} \\
\frac{\sigma_{eff}(z)}{\sigma_Y} - 1 &\leq 0 \\
0 &\leq k \leq 20 \\
8 &\leq \frac{R}{h} \leq 80
\end{aligned} \tag{19}$$

In these problems, the specific mass of structures is minimized in conjunction with maximizing the critical buckling temperature. As a constraint function, at the pre-buckling configuration, effective stress through the structures must remain at the elastic range. Moreover, decision variables are assumed to be power-law index and thinness of structures. The power-law index is considered to vary between 0 and 20. Extension of the upper-bound limit beyond the 20 seems to be unnecessary. On the other hand, the thinness of the structures is considered to alter from 8 to 80. This range is selected based on the engineering experience and the numerical data in literature.

5 Multi-Objective Improved Harmony Search Algorithm

The standard HS algorithm is conceptualized by using the musical process of searching for a perfect state of harmony. Literally, the HS is classified in a main category of optimization algorithms and a subcategory; *meta-heuristic* algorithms; and *evolutionary* algorithms. Briefly, meta-heuristics are advanced search methods for converging to the global optimum. Meta-heuristics encompass all of higher-level optimization algorithms, including the EA (evolutionary algorithms). The EAs typically mimic some natural phenomena. The core idea of EAs is the concept of evolution. In this way, the fittest and the most elite solution vectors are survivors. Since the HS uses a stochastic search instead of a gradient search, the derivative information is unnecessary. Similar to the other EAs, the HS has a set of tune parameters which are useful to deal with different decision making problems. The HS algorithm parameters are as follow:

- HM (Harmony Mmemory): The HM is a memory location where all the solution vectors

are stored as

$$HM = \begin{bmatrix} x_1^1 & x_2^1 & x_3^1 & \dots & x_N^1 \\ x_1^2 & x_2^2 & x_3^2 & \dots & x_N^2 \\ x_1^3 & x_2^3 & x_3^3 & \dots & x_N^3 \\ \vdots & \vdots & \vdots & \vdots & \vdots \\ x_1^{HMS} & x_2^{HMS} & x_3^{HMS} & \dots & x_N^{HMS} \end{bmatrix}$$

where x_n^e is the n^{th} decision variable from e^{th} solution vector.

- HMS (Harmony Memory Size): The HMS is the number of solution vectors in the HM.
- HMCR (Harmony Memory Considering Rate): The HMCR is the parameter that determines the rate of selecting new variables from stored solutions in the HM. The value of HMCR is between 0 and 1. Therefore, $(1-HMCR)$ determines the possibility of selecting new random variables from out of HM (entire possible range of decision variables). So, if x'_n is a new decision variable, it will be selected by the following procedure:

$$\begin{aligned} HMCR &\Rightarrow x'_n \in \{x_n^1, x_n^2, x_n^3, \dots, x_n^{HMS}\} \\ (1 - HMCR) &\Rightarrow x'_n \in \{x_n \mid L_n \leq x_n \leq U_n\} \end{aligned}$$

The usage of HM is important because it ensures that good decision variables stored in the HM are considered as elements of new solution vectors. If this rate is too low, only few elite variables are selected, and the algorithm may converge slowly. On the other hand, if this rate is extremely high (near 1), the decision variables in the HM are mostly used, and the other possible variables are not explored well. This condition does not lead to good solutions.

- PAR (Pitch Adjusting Rate): After choosing one of the stored decision variables (HMCR) for generating a new one, PAR determines that the selected variable is adjusted or not. The pitch adjusting means generating a new solution variable with slight changes in solution variables that are randomly selected from the HM. Therefore, if x'_n is a new selected decision variable before adjusting and x''_n is the decision variable after adjusting, the adjusting process could be indicated as

$$\begin{aligned} PAR &\Rightarrow x''_n = x'_n + A \\ (1 - PAR) &\Rightarrow x''_n = x'_n \end{aligned}$$

Here, A could be defined as $A = bw \times c$ where bw is an arbitrary band width and c is a randomly generated value that is between -1 and 1 .

- NI (Number of Improvisations): The NI determines how many times the process of improvisation should be repeated. Literary, the NI is one of the usual termination criteria in the HS algorithm.

Now, the implementation strategy of the MHS is described as follows:

- 1– *Initialize the problem*, setting the algorithm parameters, i.e. HMS, HMCR, PAR and bw .
- 2– *Initialize the HM*, the HM matrix is filled with randomly generated solution vectors.

3— *Improvise a new harmony (solution vector)*, improvisation in the HS algorithm is based on three fundamental concepts; usage of harmony memory (HMCR), pitch adjusting (PAR), and randomization (1-HMCR) [24]. The role of randomization in the HS algorithm is increasing the diversity of solutions. Although the pitch adjustment has a similar role, it corresponds to a local search. It is worth mentioning that the use of randomization can drive the system further in order to explore diverse solutions and to attain the global optimality.

4— *Update the harmony memory*, If the new solution vector is better than the worst solution vector in the HM in terms of the objective functions (new solution dominates the worst solution), the new solution is included in the HM, and the worst is discarded. This step is the main discrepancy between mono-objective and multi-objective HS algorithm. Although the sorting of solution vectors in mono-objective HS is simply performed based on one objective function, the sorting procedure in the multi-objective HS must be performed based on the pareto-optimality concept. In the same manner, obtaining the worst solution in the HM and replacing the worst solution by the new improvised solution are performed based on the pareto-optimality concept.

5— *Check the stopping criterion*, In this paper, obtaining a set of non-dominated solution vectors is the stopping criterion. As the consequence, when the developed algorithm reaches the stopping criterion, none of the solution vectors may be dominated by others. In other words, it is impossible to find the worst solution vector.

It must be noted that the mentioned steps are related to the standard MHS algorithm. In special cases the parameters of algorithm could be defined in other ways. Since the evolutionary algorithms (such as HSA) are relatively poor at yielding a precise optimum solution in a region at which the algorithm converges, the auxiliary methods such as improving, combining, and hybridizing are necessary to enhance the local search ability of evolutionary algorithms. For instance, Fesanghary et al. [45] have proposed a hybrid harmony search algorithm (HHSA) to solve mono-objective engineering optimization problems with continuous design variables.

In the present work, to enhance the local search ability of the standard harmony search algorithm, the improvisation coefficients (HMCR, PAR, and bw) have been defined dynamically [23]. Followings are the description of dynamic adjusting of improvisation coefficients. This is known that the increase in HMCR confines choosing the new solution vectors in the HM. Thus, this is equal to the increase in ability of the local search of the algorithm. Similarly, decreasing in the PAR and bw could result in rise of the local search ability for the HS algorithm. In this paper, with the increase in NI, the bw is decreased through an exponential function, PAR is decreased through a linear function, and HMCR is increased through a multiple step function. These functions are efficiently obtained based on a trial-and-error procedure which obviously is problem dependent. This means that in the process of finding the optimal pareto-points, the power of convergence is increased as the process approaches to the final iterations.

6 Results and Discussions

6.1 Validation study

In this section, the FON test function is considered for examination of the accuracy and efficiency of the proposed algorithm. The results of this study are compared with those given in reference [46]. The FON test function is defined as

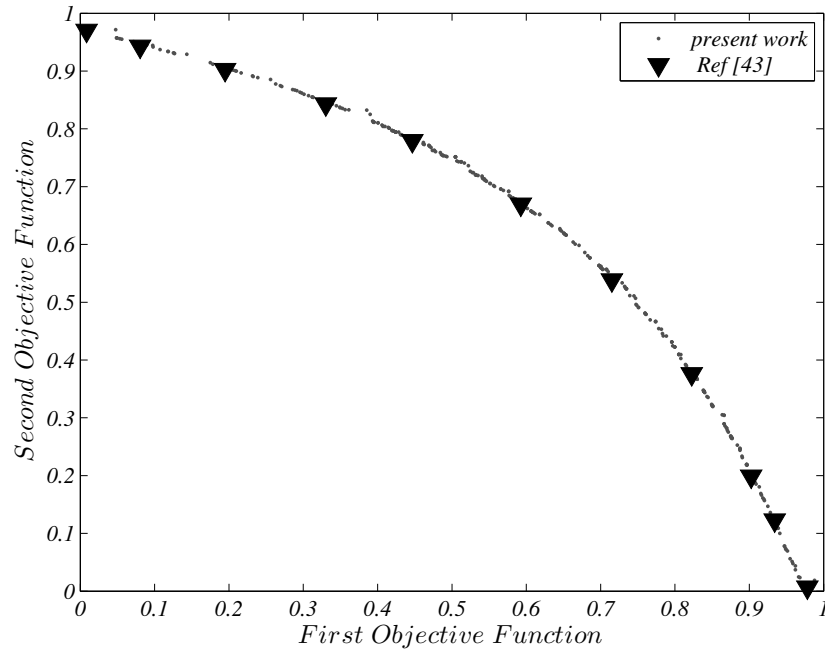


Figure 4 Pareto optimal points for FON test function.

$$f_1(x_1, x_2, x_3) = 1 - \exp\left(-\sum_{i=1}^3 (x_i - 3^{-0.5})^2\right)$$

$$f_2(x_1, x_2, x_3) = 1 - \exp\left(-\sum_{i=1}^3 (x_i + 3^{-0.5})^2\right)$$

$$-4 \leq x_1, x_2, x_3 \leq 4$$

The developed IMHSA is adopted to solve the FON test function and results are given in Fig. (4). As seen, optimal pareto-points obtained by the IMHSA are in good agreement with the results presented in reference [46]. Thus the capability of the developed algorithm is justified.

6.2 Parametric study

Consider an FG beam of length $L = 2m$ and an FG circular plate of radius $R = 2m$ at initial temperature of $300K$. Material constituents of the structures are aluminum AL and alumina AL_2O_3 . The thermo-mechanical properties of constituents are given in table (1). In table (1), $Y_m = 250Mpa$ is the yield strength of aluminum and $Y_c = 1200Mpa$ is the ultimate strength of alumina. Since these constituents have different types (Al have different alloys, and *Alumina* exist with different oxidation percent), the numerical values for the later properties are approximately selected based on data in material handbooks. According to Eq. (5) and table (1) the effective yield stress through the FGM medium is obtained as Eq. (20)

$$\sigma_y = 380.2 - 0.52V_m \quad (20)$$

According to the section 4, Eq.(20) participates in the constraint functions of optimization problems. In other words, it provides the upper bound for the effective stress at each material point of the FG structures.

Table 1 Thermo-mechanical properties of constituents [42],[43].

| | E [Gpa] | α [1/K] | k [W/mK] | ρ [kg/m ³] | Y_m [Mpa]/ U_c [Mpa] |
|--------------------------------|-----------|-----------------------|------------|-----------------------------|--------------------------|
| Al | 70 | 23.4×10^{-6} | 233 | 2707 | 250 |
| Al ₂ O ₃ | 393 | 7.4×10^{-6} | 30 | 3960 | 1200 |

The paper presents the illustrative results in the form of pareto-fronts. A pareto-front is composed of a number of solution vectors which are not dominated by each other. The number of these solution vectors is determined by the tuning parameters of the optimization algorithm. In this work, the number of solution vectors which construct the pareto-fronts is equal to the HMS. The pareto-fronts inherit the basic characteristic of the multi-objective optimization problems, *improving one of the objective functions worsens others*. This feature could be tracked through Fig. (4). As seen, solution vectors on the pareto-front are located based on their associated objective values. For the solution vectors placed on the pareto-front there may be various combinations of the objective values. In this paper the optimization problems have two objective functions, thus their associated pareto-fronts have two end-points. At these end-points the solution vectors are in their extreme conditions in the sense of objective values. That is, at the end-points of the pareto-front one of the objective functions is in its best situation and the other is in its worst situation. Moving along the pareto-front from one end-point to another one these extreme situations are reversed. For the points located between two end-points values of the objective functions are in a trade-off. This event could be clearly understood through Fig. (4). In this figure, the lower end-point belong to the maximum value of the first objective function. In this point the value of the second objective function is identically zero. Moving from this point to the upper end-point, the value of the first objective function decreases while the value of the second objective function increases. This process is continued until the value of the first objective function reaches to zero and the value of the second one reaches its maximum value. The above explanations are valid for all the pareto-fronts in general, but the arguments on the characteristic of pareto-fronts could be more extended in depth [46]. Now the results of the paper may be easily analyzed.

Figures (5) and (6), respectively, illustrate the obtained optimal pareto-points for the model problems 1 and 2. Both pareto-fronts have end-points associated with the extreme situations. Also, in both figures the horizontal axis belongs to the inverse of the critical buckling temperature and the vertical axis belongs to the specific mass of the structures. So, the lower end-point associates with the minimum buckling temperature and the minimum specific mass. As seen, moving from the lower end-point to the upper one the critical buckling temperature increases (improves) and the specific mass increases (worsens) too. These results partially satisfy the expectations; *lighter structures have lower thermal buckling resistance*.

In both model problems, some of the pareto-points have been selected for detailed considerations. These selected pareto-points have been shown in tables (2) and (3) for model problems 1 and 2, respectively.

In Tables (2) and (3), solution vectors have been sorted based on the objective values. It is obvious that an improving in one of the objective functions worsens another one. That is, the structures with higher buckling temperature have higher specific mass, and structures with lower specific mass have lower thermal buckling resistance.

Referring to the section 2, objective values have a nonlinear dependency to the decision variables. Also, decision variables affect the objective values in a non-proportional way. For instance, consider the condition in which the volume fraction of the metal phase (Al) is increased. This leads to the reduction of specific mass of the structure, at the same time the equivalent ther-

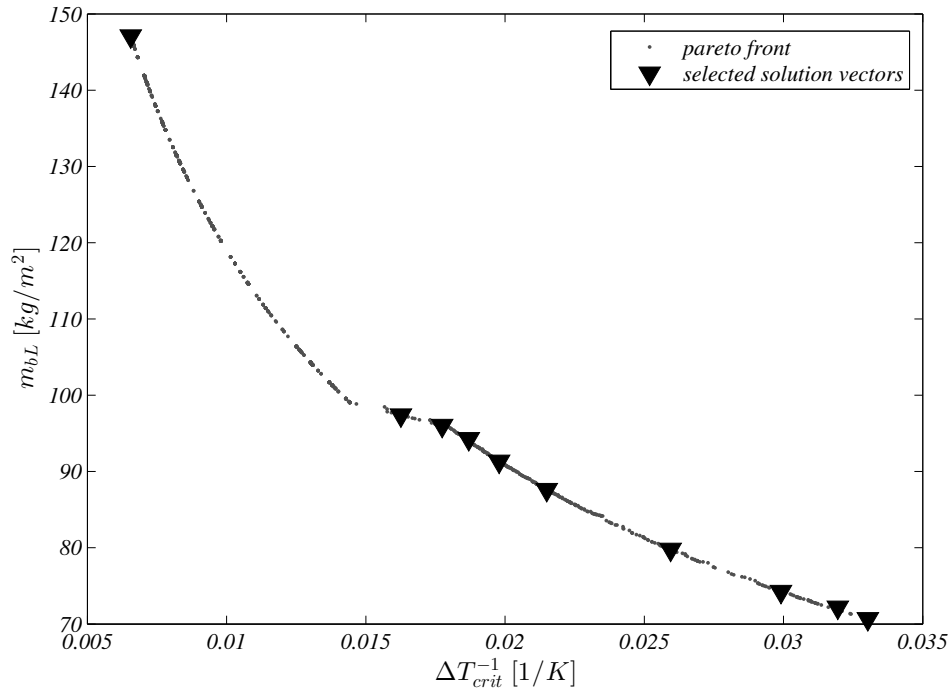


Figure 5 Pareto optimal points, optimizing FGM beams for maximum critical buckling temperature against minimum mass.

Table 2 Selective pareto optimal points and their associated objective values for model problem 1.

| | K | L/h | ΔT_{crit} | m_{bL} |
|----|--------------|--------|-------------------|----------|
| 1 | $9.26e - 04$ | 53.84 | 152.47 | 147.05 |
| 2 | 0.0574 | 79.92 | 61.49 | 97.39 |
| 3 | 0.1088 | 79.92 | 56.37 | 96.01 |
| 4 | 10.47 | 59.74 | 53.47 | 94.27 |
| 5 | 12.95 | 61.24 | 50.53 | 91.32 |
| 6 | 12.51 | 63.899 | 46.51 | 87.62 |
| 7 | 11.78 | 70.31 | 38.52 | 79.78 |
| 8 | 14.91 | 75.01 | 33.43 | 74.26 |
| 9 | 19.22 | 76.704 | 31.301 | 72.198 |
| 10 | 15.21 | 78.78 | 30.275 | 70.68 |

mal expansion of the structure increase too. The closed-form expression for the critical buckling temperature of the FG beam and the FG circular plate indicates that increasing the equivalent thermal expansion of the structures results into decrease in the critical buckling temperature. Consequently, it could be mentioned that the increasing in the volume fraction of the metal phase causes a preferred reduction in the specific mass and a non-preferred reduction in the critical buckling temperature. The later discussion hint that for a continues change in the objective values there is not a unique monotone path for changing in the decision variables. This means that for certain values of objective functions there is not exist a unique solution vector. That is, different distributions of the constituents and different structural thinness may be chosen for a desirable structural design.

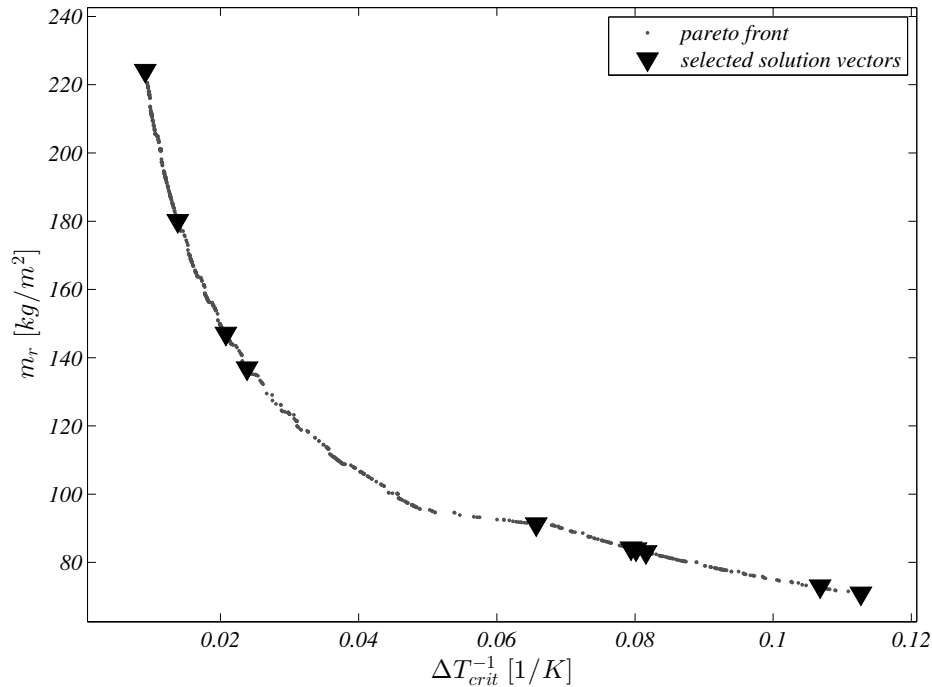


Figure 6 Pareto optimal points, optimizing FGM circular plates for maximum critical buckling temperature against minimum mass.

In this paper, based on the stochastic nature of the MHS algorithm, the pareto-optimal solutions cover a wide variety of decision variables. This property of the pareto-optimal solutions is very important in the sense of higher decision making. This is why for a certain values of objective functions, the possible solution vectors provide a selection range for decision variables. Thus, designers will be in a better position to make a choice when they face the higher level decision constraints.

Also, having a look on Tables (2) and (3), it is seen that the distribution of decision variables for the optimal pareto-points is not uniform in their possible range. This behavior for both decision variables is explainable as follows:

Power-law index: Typically, the power-law index for optimal pareto-points are in the vicinity of lower and upper bounds of possible range. These two boundary states belong to the homogeneous material distribution through the structures. When the power-law index is identically zero the material distribution is exactly homogeneous, and when the power-law index is equal to 20 the material distribution is almost homogeneous. For the homogeneous state of material distribution through the flat structures the stretching-bending coupling effect vanishes. This causes a significant reduction in thermal moment produced in the pre-buckling state. Reduction of thermal moment at pre-buckling stage results in higher buckling temperature for the flat structures. Since the higher buckling temperature is desirable for the present optimization problem, the optimal pareto-solutions are willing to have a homogeneous material distribution. For this reason the power-law indexes associated to the pareto-optimal solutions are closed to the upper/lower bound of their possible range.

Structural thinness: Although the lower structural thinness is appropriate for making further delay in thermal buckling of flat structures, the pareto-optimal solutions accept the structural thinness located in the neighborhood of its upper bound. In fact, this contradiction is due to the stress constraint of optimization problems. When the structural thinness is decreased, the thermal buckling resistance of FG flat structures is enhanced.

Table 3 Selective pareto optimal points and their associated objective values for model problem 2.

| | K | L/h | ΔT_{crit} | m_r |
|----|--------------|-------|-------------------|--------|
| 1 | 0.0128 | 33.79 | 109.79 | 224.13 |
| 2 | 0.0011 | 42.19 | 72.38 | 180.10 |
| 3 | 0.0031 | 51.62 | 48.11 | 147.11 |
| 4 | $7.33e - 06$ | 55.50 | 41.93 | 136.94 |
| 5 | 0.1607 | 80 | 15.22 | 91.22 |
| 6 | 13.0025 | 66.19 | 12.61 | 84.15 |
| 7 | 10.73 | 66.76 | 12.48 | 83.88 |
| 8 | 15.2899 | 66.80 | 12.26 | 83.07 |
| 9 | 19.74 | 75.59 | 9.36 | 73.02 |
| 10 | 17.92 | 77.97 | 8.88 | 70.92 |

This is equal to the higher pre-buckling effective stress for the thicker structures. The elevation of the pre-buckling effective stress may causes the initiation of the plastic flow at pre-buckling stage. Since the present work is confined to the range of elastic stability, the solution vectors that cause such a mentioned condition are dominated by the stress constraint function. For this reason, the pareto-optimal solutions have to accept the structural thinness near its upper bound.

7 Conclusions

This paper presents a clear monograph on the multi-objective optimization of thermal instability resistance of the FG flat structures using an IMHSA. Two model problems have been considered for this purpose. The closed-form expressions of the critical buckling temperature for the model problems have proposed in [42] and [43]. These expressions are obtained using the first-order shear deformation kinematical model, the three-parameter power-law function for material distribution, and the clamped boundary conditions. The problems have been assumed to be in the range of elastic stability. Power-law index and structural thinness have been assumed to be the decision variables. The optimization problems are defined to be the minimization of the specific mass of the structures meanwhile the maximization of the critical buckling temperature. Also, the constraint function of the problems have been defined based on the equivalent yield strength at each material point of the FGM medium. An IMHSA is developed for solving the optimization problems. The accuracy of prepared algorithm has been examined by solving the FON test function. The developed algorithm is adjusted to solve both model problems. The results have been presented in the form of pareto-optimal points for the FG beam as well as the FG circular plate. Moreover, some of the pareto-optimal solutions and their associated decision variables are tabulated. The pareto-optimal points provide a wide range of possible solutions that are useful from the design point of view. As expected, results unveil that the thinness is the crucial factor for design in the sense of elastic stability. Also, it has been found that the non-symmetric distribution of constituents are not suitable to postpone the thermal buckling of the flat FG structures.

At the end, it is worth nothing that this paper has successfully used the developed IMHSA for optimizing the thermal buckling resistance of the FG flat structures. The developed algorithm has been found a simple and accurate algorithm for optimizing the multi-objective constraint problems with continuous decision variables. The developed algorithm will be employed for

more complex optimization problems through the next works.

Acknowledgements

This work has been supported by the Iran National Science Foundations, this support is gratefully acknowledged.

The first author have a special thanks to Mr. Mohammad Komijani for his motivating suggestions on this work. Also the first author's final thanks goes to Ms. Seyedeh Elaheh Ghiasian for her helpful comments, times and efforts which are spent on this work.

References

- [1] Tanaka, K., Watanabe, H., Sugano, Y., and Poterasu, V.F., " A Multi-criterial Material Tailoring of a Hollow Cylinder in Functionally Gradient Materials: Scheme to Global Reduction of Thermo Elastic Stresses ", *Computer Methods in Applied Mechanics and Engineering*, Vol. 135, pp. 369-380, (1996).
- [2] Ootao, Y., Tanigawa, Y., and Nakamura, T., " Optimization of Material Composition of FGM Hollow Circular Cylinder under Thermal Loading: A Neural Network Approach ", *Composites: Part B*, Vol. 30, pp. 415-422, (1999).
- [3] Turteltaub, S., " Optimal Control and Optimization of Functionally Graded Materials for Thermomechanical Processes ", *International Journal of Solids and Structures*, Vol. 39, pp. 3175-3197, (2002).
- [4] Cho, J.R., and Choi, J.H., " A Yield-criteria Tailoring of the Volume Fraction in Metal-ceramic Functionally Graded Material ", *European Journal of Mechanics A/Solids*, Vol. 23, pp. 271-281, (2004).
- [5] Goupee, A.J., and Vel, S.S., " Two-dimensional Optimization of Material Composition of Functionally Graded Materials using Meshless Analyses and a Genetic Algorithm ", *Computer Methods in Applied Mechanics and Engineering*, Vol. 195, pp. 5926-5948, (2006).
- [6] Goupee, A.J., and Vel, S.S., " Optimization of Natural Frequencies of Bidirectional Functionally Graded Beams ", *Struct. Multidisc. Optim.*, Vol. 32, pp. 473-484, (2006).
- [7] Goupee, A.J., and Vel, S.S., " Multi-objective Optimization of Functionally Graded Materials with Temperature-dependent Material Properties ", *Materials and Design*, Vol. 28, pp. 1861-1879, (2007).
- [8] Vel, S.S., and Pelletier, J.L., "Multi-objective Optimization of Functionally Graded Thick Shells for Thermal Loading", *Composite Structures*, Vol. 81, pp. 386-400, (2007).
- [9] Stump, F.V., Silva, E.C.N., and Paulino, G.H., "Optimization of Material Distribution in Functionally Graded Structures with Stress Constraints", *Commun. Numer. Meth. Engng.*, Vol. 23, pp. 535-551, (2007).

- [10] Xia, Q., and Wang, M.Y., "Simultaneous Optimization of the Material Properties and the Topology of Functionally Graded Structures", *Computer-Aided Design*, Vol. 40, pp. 660-675, (2008).
- [11] Almeida, S.R.M., Paulino, G.H., and Silva, E.C.N., "Layout and Material Gradation in Topology Optimization of Functionally Graded Structures: a Globallocal Approach", *Struct. Multidisc. Optim.*, Vol. 42, pp. 855-868, (2010).
- [12] Kirikov, M., and Altus, E., "Functional Gradient as a Tool for Semi-analytical Optimization for Structural Buckling", *Computers and Structures*, Vol. 89, pp. 1563-1573, (2011).
- [13] Vatanabe, S.L., Paulino, G.H., and Silva, E.C.N., "Design of Functionally Graded Piezocomposites using Topology Optimization and Homogenization Toward Effective Energy Harvesting Materials", *Comput. Methods Appl. Mech. Engrg.*, Vol. 266, pp. 205-218, (2013).
- [14] Yas, M.H., Kamariana, S., and Poursaghar, A., "Application of Imperialist Competitive Algorithm and Neural Networks to Optimise the Volume Fraction of Three-parameter Functionally Graded Beams", *Journal of Experimental and Theoretical Artificial Intelligence*, Vol. 26, No. 6, pp. 1-12, (2014).
- [15] Taheri, A.H., Hassani, B., and Moghaddam, N.Z., "Thermo-elastic Optimization of Material Distribution of Functionally Graded Structures by an Isogeometrical Approach", *International Journal of Solids and Structures*, Vol. 51, pp. 416-429, (2014).
- [16] Birman, V., and Byrd, L.W., "Modeling and Analysis of Functionally Graded Materials and Structures", *Applied Mechanics Reviews*, Vol. 60, pp. 195-216, (2007).
- [17] Noh, Y.J., Kang, Y.J., Youn, S.J., Cho, J.R., and Lim, O.K., "Reliability-based Design Optimization of Volume Fraction Distribution in Functionally Graded Composites", *Computational Materials Science*, Vol. 69, pp. 435-442, (2013).
- [18] Loja, M.A.R., "On the Use of Particle Swarm Optimization to Maximize Bending Stiffness of Functionally Graded Structures", *Journal of Symbolic Computation*, Vol. 61-62, pp. 12-30, (2014).
- [19] Geem, Z.W., Kim, J.H., and Loganathan, G.V., "A New Heuristic Optimization Algorithm: Harmony Search", *Simulation*, Vol. 76, pp. 60-68, (2001).
- [20] Lee, K.S., and Geem, Z.W., "A New Structural Optimization Method Based on the Harmony Search Algorithm", *Computers and Structures*, Vol. 82, pp. 781-798, (2004).
- [21] Lee, K.S., Geem, Z.W., Lee, S.H., and Bae, K.W., "The Harmony Search Heuristic Algorithm for Discrete Structural Optimization", *Engineering Optimization*, Vol. 37, No. 7, pp. 663-684, (2005).
- [22] Degertekin, S.O., "Optimum Design of Steel Frames using Harmony Search Algorithm", *Struct. Multidisc. Optim.*, Vol. 36, pp. 393-401, (2008).

- [23] Mahdavi, M., Fesanghary, M., and Damangir, E., "An Improved Harmony Search Algorithm for Solving Optimization Problems", *Applied Mathematics and Computation*, Vol. 188, pp. 1567-1579, (2007).
- [24] Geem, Z.W., and Sim, K.B., "Parameter-setting-free Harmony Search Algorithm", *Applied Mathematics and Computation*, Vol. 217, pp. 3881-3889, (2010).
- [25] Degertekin, S.O., "Improved Harmony Search Algorithms for Sizing Optimization of Truss Structures", *Computers and Structures*, Vol. 92-93, pp. 229-241, (2012).
- [26] Gholizadeh, S., and Barzegar, A., "Shape Optimization of Structures for Frequency Constraints by Sequential Harmony Search Algorithm", *Engineering Optimization*, Vol. 45, No. 6, pp. 627-646, (2013).
- [27] Maheri, M.R., and Narimani, M.M., "An Enhanced Harmony Search Algorithm for Optimum Design of Side Sway Steel Frames", *Computers and Structures*, Vol. 136, pp. 78-89, (2014).
- [28] Geem, Z.W., and Hwangbo, H., "Application of Harmony Search to Multi-objective Optimization for Satellite Heat Pipe Design", *UKC AST-1.1*, (2006).
- [29] Geem, Z.W., "Multiobjective Optimization of Time-cost Trade-off using Harmony Search", *Journal of Construction Engineering and Management*, Vol. 136, No. 6, pp. 711-716, (2010).
- [30] Ricart, J., Huttemann, G., Lima, J., and Baran, B., "Multi-objective Harmony Search Algorithm Proposals", *Electronic Notes in Theoretical Computer Science*, Vol. 281, pp. 51-67, (2011).
- [31] Eslami, M.R., "*Thermo-Mechanical Buckling of Composite Plates and Shells*", Amirkabir University Press, Tehran, (2010).
- [32] Bagherizadeh, E., Kiani, Y., and Eslami, M.R., "Thermal Buckling of Functionally Graded Material Cylindrical Shells on Elastic Foundation", *AIAA Journal*, Vol. 50, No. 2, pp. 500-503, (2012).
- [33] Esfahani, S.E., Kiani, Y., Komijani, M., and Eslami, M.R., "Vibration of a Temperature-dependent Thermally Pre/post-buckled FGM Beam over a Non-linear Hardening Elastic Foundations", *Journal of Applied Mechanics*, Vol. 81, No. 1, pp. 011004, (2013).
- [34] Bateni, M., Kiani, Y., and Eslami, M.R., "A Comprehensive Study on Stability of FGM Plates", *International Journal of Mechanical Sciences*, Vol. 75, pp. 134-144, (2013).
- [35] Komijani, M., Reddy, J.N., and Eslami, M.R., "Nonlinear Analysis of Microstructure-dependent Functionally Graded Piezoelectric Material Actuators", *Journal of the Mechanics and Physics of Solids*, Vol. 63, pp. 214-227, (2014).
- [36] Bateni, M., and Eslami, M.R., "Non-linear In-plane Stability Analysis of FGM Circular

- Shallow Arches Under Central Concentrated Force”, *International Journal of Non-Linear Mechanics*, Vol. 60, No.1, pp. 58-69, (2014).
- [37] Bateni, M., and Eslami, M.R., ”Non-linear In-plane Stability Analysis of FG Circular Shallow Arches Under Uniform Radial Pressure”, *Thin-Walled Structures*, Vol. 94, No.1, pp. 302-313, (2015).
- [38] Bateni, M., and Eslami, M.R., ”Effect of Temperature Gradient on the Mechanical Buckling Resistance of FGM Shallow Arches”, *ASME 2014 12th Biennial Conference on Engineering Systems Design and Analysis*, pp. V001T01A006-V001T01A006, (2014).
- [39] Tamura, I., Tomota, Y., and Ozawa, H., ”Strength and Ductility of FeNiC Alloys Composed of Austenite and Martensite with Various Strength”, *Proceedings of the Third International Conference on Strength of Metals and Alloys*, Vol. 1, pp. 611-615, (1973).
- [40] Williamson, R.L., Rabin, B.H., and Drake, J.T., ”Finite Element Analysis of Thermal Residual Stresses at Graded Ceramic Metal Interfaces. Part I. Model Description and Geometrical Effects”, *Journal of Applied Physics*, Vol. 74, No. 2, pp. 1310-1320, (1993).
- [41] Jin, Z.H., and Dodds Jr, R.H., ”Crack Growth Resistance Behaviour of a Functionally Graded Material: Computational Studies”, *Engineering Fracture Mechanics*, Vol. 71, pp. 1651-1672, (2004).
- [42] Kiani, Y., Rezaei, M., Taheri, S., and Eslami, M.R., ”Thermo-electrical Buckling of Piezoelectric Functionally Graded Material Timoshenko Beams”, *International Journal of Mechanics and Materials in Design*, Vol. 7, pp. 185-197, (2011).
- [43] Najafizadeh, M.M., and Eslami, M.R., ”First-order-theory-based Thermoelastic Stability of Functionally Graded Material Circular Plates”, *AIAA Journal*, Vol. 40, No. 7, pp. 1444-1450, (2002).
- [44] Geem, Z.W., ”*Music-inspired Harmony Search Algorithm Theory and Applications*”, Springer-Verlag Berlin Heidelberg, (2009).
- [45] Fesanghary, M., Mahdavi, M., Minary-Jolandan, M., and Alizadeh, Y., ”Hybridizing Harmony Search Algorithm with Sequential Quadratic Programming for Engineering Optimization Problems”, *Computer Methods in Applied Mechanics and Engineering*, Vol. 197, pp. 3080-3091, (2008).
- [46] Deb, K., ”*Multi-objective Optimization Using Evolutionary Algorithms*”, John Wiley Sons Ltd., England, (2001).

چکیده

مقاله حاضر به صورت روشن و صریح به بهینه‌سازی مقاومت سازه‌های مسطح ساخته شده از مواد هدفمند در مقابل ناپایداری سازه‌ای تحت بار حرارتی می‌پردازد. برای این منظور دو نمونه سازه در نظر گرفته شده‌اند که عبارتند از: یک تیر ساخته شده از مواد هدفمند و یک ورق گرد ساخته شده از مواد هدفمند. فرض شده است که این سازه‌ها از مواد هدفمند با توابع توزیع سه متغیره ساخته شده‌اند، از مدل برشی مرتبه اول تبعیت می‌نمایند و دارای تکیه‌گاه گیردار می‌باشند. توابع هدف برای مسئله بهینه‌سازی حاضر حداکثر سازی دمای بحرانی کمانش در حین حداقل سازی وزن سازه‌ها در نظر گرفته شده است. همچنین با در نظر گرفتن توابع قید مناسب، مسئله به محدوده پایداری الاستیک سازه‌ها محدود شده است. مقاله حاضر برای مسئله مطرح شده یک الگوریتم بهینه‌سازی جستجوی هارمونی چند هدفه بهبود یافته پیشنهاد می‌کند. توانایی الگوریتم ارائه شده با حل یک مسئله بهینه‌سازی شناخته شده تایید می‌گردد. نتایج گرافیکی در غالب نقاط بهینه پرتو برای مسائل مطرح شده نمایش داده می‌شوند و تعدادی از این نقاط با جزئیات کامل در جدول‌هایی ارائه می‌گردند. نتایج نشان می‌دهند که توزیع نامتقارن مواد در راستای ضخامت سازه‌های تخت برای افزایش دمای بحرانی این سازه‌ها مناسب نمی‌باشد.